ACS OMEGA

Open Access



http://pubs.acs.org/journal/acsodf

Article

# Mechanistic Modeling of Size Exclusion Chromatography-Assisted *In Vitro* Refolding of the Recombinant Biosimilar Teriparatide (PTH-34)

Santosh Ughade, Sunil Rana, Mohd Nadeem, Rupali Kumthekar, Sanjay Mahajani, and Rahul Bhambure*

Cite This: *ACS Omega* 2024, 9, 3204−3216

Read Online

ACCESS | Metrics & More | Article Recommendations | Supporting Information

**ABSTRACT:** *In vitro* protein refolding is one of the critical unit operations in manufacturing recombinant peptides expressed using *Escherichia coli* as host cells. This study is focused on designing size exclusion chromatography-assisted *in vitro* refolding process for biosimilar recombinant parathyroid hormone. Inclusion bodies (IBs) of recombinant parathyroid hormone were solubilized at higher pH, and *in vitro* refolding was performed using size exclusion chromatography. In the first part of the investigation, DoE-based empirical optimization was performed to achieve a higher refolding yield for a biosimilar recombinant parathyroid hormone. The effect of solubilized inclusion body (IB) feed volume, concentration of IBs, and residence time on *in vitro* refolding of recombinant teriparatide was studied using the Box−Behnken design. Size exclusion chromatography (SEC)-assisted *in vitro* refolding was performed at 8 °C at pH 10.5 by using 20 mM Tris buffer. The maximum refolding yield of 98.12% was achieved at feed volume (12.5% of CV) and 20 mg/mL inclusion body (IB) concentration with a residence time of 50 min and a purity of 66.1% based on densitometric analysis using SDS-PAGE. In the latter part of the investigation, the general rate mechanistic model framework for size exclusion chromatography was developed and validated with the experimental results. The developed model helped in the accurate prediction of the elution volumes and product yield. The developed model also helps to predict the elution performance of a scalable column a priori. Post *in vitro* refolding, the formation of the native peptide structure was examined using various orthogonal analytical tools to study the protein's primary, secondary, and tertiary structures. The developed hybrid process development approach is a valuable tool toachieve high-yield, scalable refolding conditions for recombinant proteins without disulfide bonds.

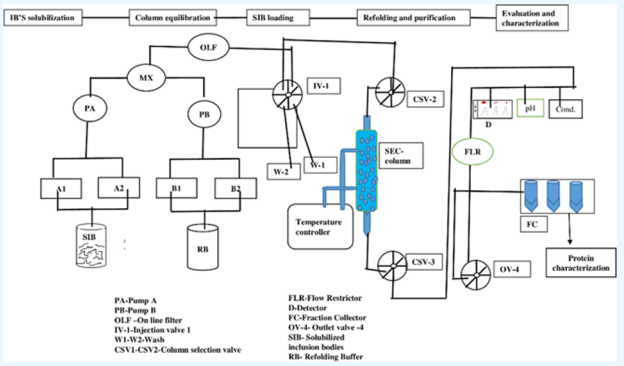


## 1. INTRODUCTION

Therapeutic peptides are a distinct class of biotherapeutics that are polyamide polymers made up of 50 amino acid residues with molecular mass ranges from 500 to 5000.[1] These therapeutic peptides predominantly function as hormones, neurotransmitters, growth factors, anti-infective agents, or ion channel ligands. Like recombinant monoclonal antibodies (mAbs), peptides bind cell surface receptors with high specificity and affinity and exert their effect.[2] Since 1920, when the treatment of diabetes was altered by the consumption of insulin produced by animals such as pigs and cows, biologically active peptides have been used for various medicinal purposes.[3] The completion of 100 years of using insulin therapy in 2021 was a significant event highlighting the advancement of peptide-based therapeutics.[4] Since then, more than 80 therapeutic peptide drugs have been introduced globally.[5] Research into new peptide-based therapeutics continues steadily with more than 150 peptides in clinical development and around 400−600 peptides undergoing preclinical studies. Because they may target protein−protein interactions, which were once difficult for pharmaceuticals, peptides have become increasingly prevalent[6] with a higher success rate in clinical trials than others. Peptides are also cost-effective compared to biologics such as mAb's, antibody-based, and other therapeutics.[7] They are highly potent and specific and have low toxicity, making them valuable in drug discovery and development.[8]

Commercially, various host systems are used for the production of biotherapeutic peptides, such as bacteria (such as *Escherichia coli*), yeast (such as *Pichia pastoris*), and mammalian cells (such as CHO and NS0).[9,10] The most favored host system for expression, nevertheless, is bacteria. This is because *E. coli* reproduces quickly, produces a high product, is efficient in terms of cost, and has a simple process to scale.[11,12]

**Received:** June 23, 2023
**Revised:** December 10, 2023
**Accepted:** December 21, 2023
**Published:** January 5, 2024

However, *E. coli*-based therapeutic peptide expression leads to the formation of inclusion bodies (IBs) due to overexpression and inadequate refolding conditions, such as a lack of sufficient cell folding mechanisms. This causes the protein molecule to remain unfolded or partially folded, forming aggregates referred to as IBs.[13] As a result, the therapeutic peptides must be refolded into their unique three-dimensional structure, which is critical during the recovery of a bioactive protein. The traditional approach to recovering active protein IBs includes four significant steps: cell lysis, isolation and purification of IBs, solubilization of IBs, and refolding and purifying functional proteins utilizing different chromatographic techniques.[14] Various refolding methods have been reported, such as dilution, dialysis, diafiltration, chaperone-assisted refolding, low-molecular-weight additive-assisted refolding, and refolding by chromatography.[15,16] Among these techniques, dilution-based methods are the most widely used *in vitro* method for refolding proteins from IBs.[17,18]

To refold the proteins using the dilution method, purified inclusion bodies need to be solubilized in chaotropic agents such as 6 M GdHCl, 8 M urea, or alkaline pH, with reducing agents such as dithiothreitol or $\beta$-mercaptoethanol. This helps denature the IB-aggregated structure and opens up the protein's primary structure.[19] The denatured and reduced IBs are then slowly added into an oxidizing environment with a stabilizer to favor their native protein conformation. After incubation, the protein is clarified, concentrated, and diafiltered against a chromatography equilibration buffer using an ultrafiltration system.[20,21] However, this method has a low refolding yield and product recovery, leading to high costs and downstream bottlenecks. Proteins are often refolded at low concentrations in large stirred tanks to achieve higher yields and reduce protein aggregation, limiting downstream throughput and facility fit.[22] To address this challenge, biopharmaceutical industries seek more efficient refolding methods to improve product recovery and reduce manufacturing costs, such as high throughput ultrafiltration and diafiltration processes to reduce the process volume and intensify downstream processes, ultimately increasing the overall downstream process yield.

Improving the efficiency of large-scale protein refolding processes at higher protein concentrations has been one of the critical research areas in the past decade. Chromatography-assisted *in vitro* refolding approaches have been developed to address this issue. On-column protein refolding can be achieved using ion exchange chromatography, size exclusion chromatography, and metal affinity chromatography.[23,24] Chromatography-assisted protein refolding is advantageous over dilution-based refolding, as it can separate contaminants, quickly remove denaturants, and refold the recombinant proteins at higher concentrations. Many reports have shown that size exclusion chromatography can be extensively used as a refolding tool for various model proteins expressed in the form of inclusion bodies (IBs).[25] It has been hypothesized that using size exclusion chromatography for protein folding reduces aggregate formation by gradually removing denaturants and separating folding intermediates due to different diffusion properties while passing through the column.[22] Boris et al. showed in their report that hen egg white lysozyme was refolded using size exclusion chromatography; when the initial load concentration was low, the aggregation reaction for lysozyme was reduced; however, with a higher concentration load, an elevated aggregation reaction was observed.[26] Gao et al. in their investigation found that a lower initial concentration of the IBs is associated with a higher refolding yield with high specific activity.[27] During *in vitro* refolding of inclusion bodies, it is found that the formation of the aggregates is more prone when the local denatured protein concentration exceeds a critical concentration, which ultimately influences the recovery of active proteins.[28] To mitigate protein aggregation during refolding, urea gradient size exclusion chromatography was developed. Urea gradient size exclusion chromatography (UGSEC) was initially introduced to refold egg white lysozyme by Gao Yong-gui et al. The experiment utilized a prepacked Superdex 75 (10/30) column with a urea concentration of 2 M as the final plateau concentration and a urea gradient length of 6 mL. The refolding efficiency was compared among UGSEC, typical SEC, and dilution methods. The results indicated that UGSEC yielded a higher activity recovery than the other two methods.[29] Additionally, the difference in activity recovery between gradient refolding and the other two methods was more significant for higher initial protein concentrations.[30,31]

In this study, we used a size exclusion chromatography-based approach for *in vitro* refolding recombinant teriparatide and simulated the elution behavior inside the size exclusion chromatography column. It consists of 34 amino acids with a molecular weight of 4117.8 Da.[32] Overexpression of recombinant teriparatide using *E. coli* leads to the formation of IBs. Consequently, it must be denatured, solubilized using a chaotropic agent, and refolded in its native folded state. To design a robust size exclusion chromatography-based refolding method for teriparatide with minimal protein aggregation, we have used a DoE-based approach for refolding optimization. Residence time (min), feed volume (% CV), and solubilized IB concentration (mg/mL) were considered critical process parameters that could affect the yield of the refolding process. MATLAB code was developed based on a general rate model and used to simulate the elution behavior of teriparatide inside the size exclusion chromatography column under varying operating conditions. The effect of critical process parameters like initial IB concentration, residence time, and feed volume (% CV) was evaluated. Post refolding, the native structure of biosimilar teriparatide was studied using various orthogonal analytical tools, such as reverse phase HPLC, SDS-PAGE, fluorescence spectroscopy, and LC-ESI-MS/MS MALDI-TOF, at the primary level of analysis. Additionally, MS-based techniques were utilized to verify the intact protein's amino acid sequence. The research also assessed collision-induced dissociation (CID)-based fragmentation techniques to map the teriparatide.

**1.1. Theory and Mathematical Modeling of Size Exclusion Chromatography for *In Vitro* Refolding.** Size exclusion chromatography (SEC) is a commonly used technique for separating and analyzing biomolecules based on their size. The method involves using a stationary phase with pores of varying sizes, which allow smaller biomolecules to enter and be retained for a more extended period. In comparison, larger biomolecules are excluded and eluted earlier. The mobile phase, typically a buffer solution, transports the biomolecules through the column. To better understand the separation process in SEC, mathematical models have been developed.[27] These models describe the biomolecules' behavior and the column's mobile phase. They can predict the elution behavior of different biomolecules under different SEC conditions. This model helps to predict the elution behavior of biomolecules of different sizes under other SEC conditions.


https://doi.org/10.1021/acsomega.3c04463
ACS Omega 2024, 9, 3204−3216

The general rate model used in size exclusion chromatography considers three key mass transfer processes within the column. These processes are as follows.

1. Axial dispersion within the bulk fluid phase describes the spreading of the solutes as they move down the column due to the effects of diffusion and convection.
2. Interfacial film mass transfer between the stationary and mobile phases refers to the transfer of solutes between the two phases as they come into contact.
3. Diffusion of protein molecules within the solid phase refers to the movement of the solutes through the pores of the stationary phase due to differences in concentration. These processes all play a role in determining the rate of separation and elution of solutes within the SEC column.

The governing equations for mass balances for a solute in the bulk and particle phases, respectively, are as follows.

$$\frac{\partial C_b}{\partial t} = D_{ax}\frac{\partial^2 C_b}{\partial z^2} - v\frac{\partial C_b}{\partial z} - \frac{3k_f(1-\varepsilon_b)(C_b - C_{p,R=R_p})}{\varepsilon_b R_p} \quad (1)$$

$$\frac{\partial C_p}{\partial t} = D_p\left(\frac{\partial^2 C_p}{\partial z^2} + \frac{2}{R}\frac{\partial C_p}{\partial R}\right) \quad (2)$$

The partial differentials in eqs 1 and 2 are subject to the following initial and boundary conditions. The Danckwerts boundary conditions were used at the inlet and outlet of the column.

**Initial conditions:**

At $t = 0$

$$C_b = C_b(0, R, z)$$

$$C_p = C_p(0, R, z)$$

**Boundary conditions:**

At $z = 0$

$$\frac{\partial C_b}{\partial z} = \frac{v}{D_{ax}}[C_b - C_0(t)]$$

At $z = L$

$$\frac{\partial C_b}{\partial z} = 0$$

At R = 0

$$\frac{\partial C_p}{\partial z} = 0$$

At R = $R_p$

$$\frac{\partial C_p}{\partial R} = \frac{k_f}{\varepsilon_p}(C_b - C_{p,R=R_p})$$

*1.1.1. Model Parameter Estimation Using the Inverse Fitting Method.* The mass transfer parameters, including the axial dispersion coefficient (Dax), film mass transfer coefficient (Kf), and pore diffusion coefficient (Dp), are crucial in describing the behavior of the general rate model (GRM). To determine the appropriate mass transfer parameters, the experimental chromatogram was compared against the numerical solutions of partial differential equations (eqs 1 and 2), with the residual minimized to obtain the best-fit parameters. The model parameter estimation is a critical step in developing any mathematical model for various physical systems. The primary objective of parameter estimation is to identify the set of parameters p that best represents the underlying physical phenomena of a system. The process of parameter estimation involves comparing the model predictions ($c_{sim}(p, t)$) against a set of experimental measurements ($c_{exp}(p, t)$). In particular, the aim is to find the values of $p$ that minimize the discrepancy between the model predictions and experimental data. Typically, the experimental data consist of $N_m$ measurements, each comprising $N_{p,j}$ data points obtained at time points $t_i^{(j)}$, $i = 1, 2, 3,...N_{p,i}$, $j = 1, 2, 3,....N_m$. These measurements are compared against the corresponding simulation data generated by the model, and the difference between the two sets of data is summarized by the least-squares residual. The least-squares residual measures how well the model predictions fit the experimental data. It is calculated as the sum of the squared differences between the experimental measurements and the corresponding model predictions (eq 3).

$$res(p) = \sum_{j=1}^{N_m}\sum_{i=1}^{N_p}[c_{sim}(p, t_i^{(j)}) - c_{exp,i}^{(j)}]^2 \quad (3)$$

This optimization process was carried out using MATLAB's lsqnonlin optimizer, a widely used optimization tool for nonlinear least-squares problems. The exact parameter sensitivities were calculated by CADET, a software package designed for simulating chromatographic processes. A MATLAB script was developed and integrated into the CADET framework to automate the formulation and calculation of the residual. This helped to streamline the optimization process and improve the efficiency of parameter estimation. Furthermore, parameter transformations were used to reduce the error due to different orders between parameters and bring all parameters to the same scale. Scaling is important for the performance of the optimizer, since it directly influences the sensitivity inside the optimizer. Here, a logarithmic transformation to each parameter was applied in order to remove the different scales (see eq 4).

$$p_i^T = \ln(p_i) \quad (4)$$

Here, $p_i^T$ and $p_i$ are transformed and actual parameters, respectively.

## 2. MATERIALS AND METHODS

**2.1. Chemicals.** *Escherichia coli* strain BL21(DE3) was purchased from Novagen (Merck Life Science Pvt Ltd., India). Tartoff- Hobbs HiVeg terrific broth (Cat. No. MV1250-500 G), Miller Luria−Bertani HiVeg broth (Cat. No. MV1245-500 G), kanamycin sulfate (Cat. No. CMS210-5G), glycerol for molecular biology (Cat. No. MB060-1 L), and isopropyl β-D-1-thiogalactopyranoside (IPTG) were purchased from HiMedia, India. Tris ultrapure grade (Cat. No. 103133-1KG) was purchased from MP Biomedicals. L-Arginine (Cat. No. TC052-1KG) was purchased from HiMedia, India. Acetonitrile (Cat. No. 0990-55) was purchased from Thomas Baker Private Limited, India. Trifluoracetic acid (LR), bromophenol blue (Cat. No. B8026-25 G), β-mercaptoethanol (Cat. No. M3148-250 ML), glycine (Cat. No. G8898-1KG), ammonium persulfate (Cat. No. A3678- 100 G), sodium dodecyl sulfate (Cat. No. L3771-1KG), bis(acrylamide) (Cat. No. M7279-250 G), ethylenediaminetetraacetic acid disodium salt dihydrate (Cat. No. E5134-500 G), *N*,*N*,*N*′,*N*′-tetramethylethylenedi-


https://doi.org/10.1021/acsomega.3c04463
ACS Omega 2024, 9, 3204−3216

amine (Cat. No. T9281-100 ML), hydrochloric acid (Cat. No. 339741-500 ML), TEV protease (In-house from NCL, Pune), formic acid (LC-MS grade, Fluka), leucine enkephalin (Waters Corp), and VL16 (Vantage L Laboratory Column VL 16 × 250, Darmstadt, Germany) were used.

**2.2. Equipment.** Bacterial cell separation was achieved using an Eppendorf 5804R refrigerated centrifuge (Germany). A high-pressure homogenizer, GEA Lab Homogenizer Panda PLUS 2000 (GEA Niro Soavi), was used for mechanical cell disruption. Protein concentration was measured using UV−visible spectrophotometry (Nanodrop 2000, Thermo Scientific). A refrigerated/heated circulator water bath (manufactured by Julabo GmbH in Germany) was used to control the temperature of the refolding buffer present in a jacketed glass vessel during the on-column refolding. A VL16 column was used for on-column refolding of teriparatide using size exclusion chromatography. Reversed-phase high-performance liquid chromatography (RP-HPLC) analysis for expressed and refolded recombinant teriparatide measurement was carried out with a Phenomenex Widepore XB-C18 analytical 4.6 mm × 150.0 mm 5.0 $\mu$m (Phenomenex), operating with an Agilent 1260 HPLC system (Agilent Technologies). ÄKTA Pure 150 (GE Healthcare Life Sciences) systems were used to perform the on-column refolding experiment of peptides (PTH 1−34), and UNICORN 7.0 software was used to monitor the system. A SYNAPT XS (Waters Corp) mass spectrometer was equipped with an ACQUITY UPLC I-Class PLUS system. Data acquired on SYNAPT XS (Waters Corporation) were analyzed using UNIFI v1.9.4.053 (Waters Corporation).

**2.3. Cloning and Expression of Recombinant Teriparatide at the Shake Flask and Bioreactor Level.** The gene constructs for recombinant teriparatide were chemically synthesized and inserted into the pET-30b (+) vector (made by Novagen in Germany). T7-based promoter expression vector pET30b (+) DNA was constructed by cloning a recombinant teriparatide coding nucleotide sequence at the 5′ end into NdeI and XhoI restriction for protein expression. *E. coli* BL21 (DE3) cells were transformed with the recombinant pET30b DNA vector containing the recombinant teriparatide gene sequence to check the protein's expression efficiency in the host cell. To confirm the transformation efficiency of the plasmid carrying recombinant teriparatide gene, the LB kanamycin agar plates were at a final concentration of 30.0 $\mu$g/mL. From the colony PCR results, the positive transformed colonies were selected and subcultured in terrific HiVeg broth with 30.0 $\mu$g/mL kanamycin to check the expression of teriparatide. The cells were incubated at 37.0 °C and 225 rpm. The target was expressed by using 1 mM IPTG as an inducer and incubated at 37.0 °C. The overnight cultured cells were harvested by centrifugation at 6000 rpm for 20.0 min. The protein expression was confirmed using SDS-PAGE in reducing conditions. After confirmation of the recombinant teriparatide (1−34) expression at the shake flask level, the next step was to conduct cultivations at the bioreactor level. Bioreactor cultivation was done at 37.0 °C in a 2 L reactor, using a working volume of 1 L. To start the fermentation at a 1 L scale, 1 absorbance at 600 nm 10% seed culture was added to 900 mL medium. After reaching an absorbance of 20 at 600 nm, the culture was induced with 1 mM IPTG, and the time post induction was determined by constant absorbance and the culture harvested. The culture was collected. Cell biomass was separated by centrifugation.

**2.4. Cell Lysis and Solubilization of Inclusion Bodies.** The harvested cell biomass was resuspended in lysis buffer A (20.0 mM Tris, 0.3 M NaCl, 2 mM EDTA, pH 9.0), and cell disruption was performed using a high-pressure homogenizer (3 passes 600 bar pressure) for 30.0 min, and the IBs were isolated by centrifuged at 8000 rpm for 30.0 min at 4.0 °C from cell lysate. The inclusion bodies were subjected to multiple washing steps to remove impurities, such as host cell proteins and nucleic acid. In the first step, lysed cells were washed with lysis buffer B (A containing 2.0 M urea). In the second washing, step cells were washed with lysis buffer C (lysis buffer A containing 1.0% Triton X-100). Finally, the cells were washed with 20.0 mM Tris base and 2.0 mM EDTA, pH 9.0, to purify IBs. The IBs were stored at −20.0 °C until further use. Purified IBs were solubilized for 2 h in a solubilization buffer (20 mM Tris base, 2.0 mM EDTA, pH 12.5). Post solubilization, the mixture was centrifuged at 10,000 rpm for 15.0 min at 10 °C. The supernatant was collected, and absorbance at 280 nm was measured. Solubilized recombinant teriparatide IB concentration was measured using RP-HPLC.

**2.5. *In Vitro* Size Exclusion Chromatography-Assisted Refolding of Recombinant Teriparatide.** The purified recombinant teriparatide IBs were subjected to solubilization using buffer containing 20 mM Tris base and 2.0 mM EDTA, pH 12.5, at different IB concentrations such as 20, 25, and 30 mg/mL and solubilized at room temperature (25.0 ± 2.0 °C) for 2 h. Sephadex G-25 was packed in a VL16 column with a bed height of 25 ± 0.5 cm. Post column packing, a series of standard tests were conducted to evaluate performance and qualify the column. The column was qualified using pulse response experiments by injecting 1 M NaCl into the column and 10 mg/mL blue dextran by injecting a 25% column volume (50 mL). The peaks were evaluated by using the numerical integration method. After the column qualification, the column was equilibrated with the refolding buffer, which contained 20 mM Tris base, 2.0 mM EDTA, and 0.2 M arginine hydrochloride (pH 10. 5). The solubilized IBs were centrifuged, and the supernatant was injected in a Sephadex G-25 SEC column. The refolding experiment was performed at 8 °C (8.0 ± 1.0 °C) for 50, 75, and 100 min. Refolded recombinant teriparatide (PTH-34) was eluted, and the fractions were collected. Fractions of recombinant teriparatide loaded on 15% SDS-PAGE electrophoresis under reducing and nonreducing conditions, and SDS-PAGE was run at 70 constant voltages. All fractions were collected from the size exclusion chromatography, and the buffer was exchanged with phosphate buffer pH 7.4. For the conversion of recombinant teriparatide (PTH-78) to recombinant teriparatide (PTH-34), we used the TEV protease enzyme-based digestion, which cleaves the ENFLYQ(G/S) amino acid sequence. The ratio of TEV to the recombinant teriparatide precursor was optimized and finally used in a 1:10 ratio. The TEV protease-based digestion was performed at room temperature for 4 h.

**2.6. Analytical Characterization of Refolded Recombinant Teriparatide.** *2.6.1. Quantitative Determination of Refolded Teriparatide Using HPLC Analysis.* High-performance liquid chromatography was used to measure the concentration of teriparatide, which was recovered from size exclusion chromatography-based refolding. An Agilent 1260 LC system was used for the measurement at a 215 nm wavelength. Two mobile phases were used to separate protein mobile phase A (0.1% TFA + Milli-Q water) and mobile phase B (0.1% TFA + acetonitrile). A reversed-phase C18 column was used (4.6 mm, 250 mm, particle size 5 $\mu$m, and porosity 300 Å). The protein separation was done by a gradient-based method with a flow rate


https://doi.org/10.1021/acsomega.3c04463
ACS Omega 2024, 9, 3204−3216

of 1 mL/min and a temperature of 45 °C. Various concentration ranges (0.1, 0.2, 0.3, 0.4, and 0.5 mg/mL) were chosen to determine the refolded teriparatide linearity. Three injections of 20 $\mu$L of each concentration were used to determine the average peak area based on linearity for each concentration. The concentration curve was then fitted to the straight-line equation. To calculate the total recovery of recombinant teriparatide, the average loaded sample area and the area of the all-fractionated sample were fitted into the equation.

*2.6.2. Fluorescence Analysis of Refolded Recombinant Teriparatide.* The intrinsic fluorescence of refolded recombinant teriparatide was compared with the internal reference standard using an FP 8300 JASCO fluorescence spectrophotometer. Emission spectra were captured from the 200−400 nm range, and excitation was kept at 295 nm. The excitation and emission wavelength slit widths were set to 2.5 nm for each sample, and data were collected in triplicates. The response from fluorescence spectroscopy was recorded as wavelength versus absorbance.

*2.6.3. Intact Mass Analysis of Refolded Recombinant Teriparatide Using Matrix-Assisted Laser Desorption/Ionization (MALDI-TOF).* Matrix-assisted laser desorption/ionization was used to perform an intact mass analysis of purified refolded recombinant teriparatide. The matrix used was sinapic acid (10 mg/mL with 50% acetonitrile, 50% LC-MS grade water, and 0.1% trifluoroacetic acid). 1 mL of this diluted solution was then spotted on a MALDI plate and allowed to crystallize in a metal plate. The sample was analyzed using a MALDI-TOF, AB SCIEX TOF/TOF 5800 in linear mode with 6000−7000 laser shots being accumulated to produce a spectrum. The width of the mass window for the recombinant teriparatide spectrum was set to 500− 10000 Da for precursor ions with a mass greater than 500 Da and less than 10000 Da for with or without tag teriparatide molecules. MS/MS data were obtained using the instrument's default calibration without internal or external calibration.

*2.6.4. Amino Acid Sequence Identification and Confirmation of Refolded Teriparatide and Reference Standard.* Refolded recombinant teriparatide (1−34) samples were buffer-exchanged into 50 mM ammonium bicarbonate (pH: 7.8 and conductivity 5.14 mS/cm). A Sephadex G-25 desalting column (CV: 5 mL) was connected to a KTA pure 150 and operated at a 2 mL/min flow rate. Before sample application, the column was equilibrated with a desalting buffer (50 mM ammonium bicarbonate). Protein concentration was measured by UV−visible spectrophotometry (NanoDrop 2000/2000c spectrophotometer), and 50 mM ammonium bicarbonate was used for buffer exchange of all of the samples. The final concentration of protein samples was kept constant at 1 mg/mL for intact mass and peptide mapping. Samples were analyzed on a SYNAPT XS (Waters Corp) mass spectrometer equipped with an ACQUITY UPLC I-Class PLUS system. The mass spectrometer was calibrated using sodium iodide (MS grade, Waters Corp) over 400−4500$m/z$ for intact mass analysis and over 50−2000$m/z$ for peptide mapping. Additionally, 50 fmol/$\mu$L leucine enkephalin (Waters Corp) at a flow rate of 5.0 $\mu$L/min was used as the Lock-Mass (556.2771 $m/z$, singly charged, positive mode) during the data acquisition, and mass correction was applied during data processing. Leucine enkephalin was infused through an independent port (LockSpray), and the Lock-Mass was recorded once every 40 s. The switch from survey scan to MS/MS was performed when the intensity of the precursor ion increased at a rate of 7500 counts/second. Data acquired on the SYNAPT XS (Waters Corporation) was analyzed using UNIFI v1.9.4.053 (Waters Corporation).

## 3. RESULTS AND DISCUSSION

**3.1. High Cell Density Fermentation of E. coli to Produce Recombinant Teriparatide (PTH).** Biosimilar recombinant teriparatide was expressed using *E. coli* BL21 (DE3) as a host system. The expression was carried out by cloning the protein-coding sequence in the pET-30b expression vector. The recombinant teriparatide protein was expressed as an IB with a molecular weight of 9.0 kDa (teriparatide sequence with additional signal sequence) and comprised 78 amino acids. The *E. coli* cells were grown at 37 °C and induced with 1 mM IPTG for 8 h in a 100 mL shake flask. However, the protein was expressed in the form of inclusion bodies (IBs), which were then isolated and purified. The purified IBs were dissolved in the solubilization buffer (0.02 M Tris base and 2 mM EDTA pH 12.5), and SDS-PAGE was performed to check the recombinant teriparatide expression. Figure 1A depicts the expression of recombinant teriparatide in the form of IBs. Post confirmation at the shake flask level, the protein was overexpressed for the *in vitro* refolding study at the bioreactor level. Bioreactor cultivation was performed at 37.0 °C in a 2 L reactor with a working volume of 1 L. To start the fermentation at the 1 L scale, 10% of seed culture was added to 900.0 mL of media in the bioreactor. IPTG was used as an inducer for the expression of recombinant teriparatide in *E. coli*. Post-induction time was decided based on absorbance at 600 nm, and the cells were harvested using centrifugation at 6000 rpm for 30 min at the temperature of 10 °C. The resulting cell biomass was then mixed with lysis buffer at a ratio of 1:10 (w/v) and mechanically disrupted using a high-pressure homogenizer for three passes at 600 bar. The resulting lysate was centrifuged at 10,000 rpm for 30 min at 4 °C to obtain the IBs in the pellet. The IBs underwent a three-step washing protocol to remove impurities using different solutions using different chemical additives such as urea and Triton X-100. The washed IBs were stored at −20 °C for future use. The moisture content of the purified IBs was

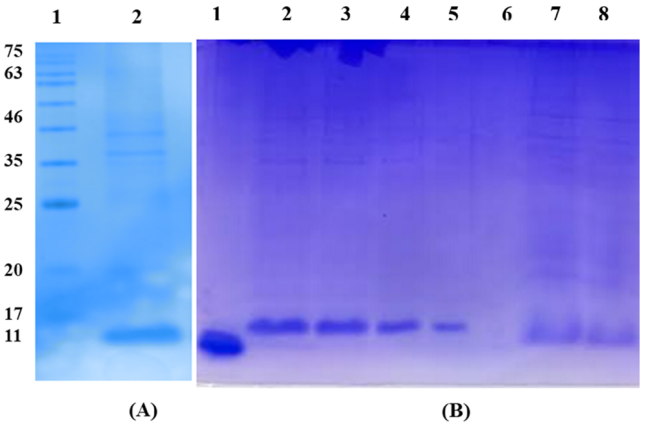


**Figure 1.** SDS-PAGE analysis of recombinant teriparatide expressed under reducing conditions; [(A) Lane 1—protein marker and Lane 2—undigested solubilized teriparatide (molecular weight of 9 kDa) and (B) Lane 1—reference standard Teriparatide (molecular weight of 4.1 kDa), Lane 2 and Lane 3: solubilized IBs of recombinant teriparatide, Lane 4 and Lane 5—SEC eluted undigested teriparatide, Lane 6—empty, and Lane 7 and Lane 8—digested teriparatide showing a molecular weight of 4.1 kDa].


https://doi.org/10.1021/acsomega.3c04463
ACS Omega 2024, 9, 3204−3216

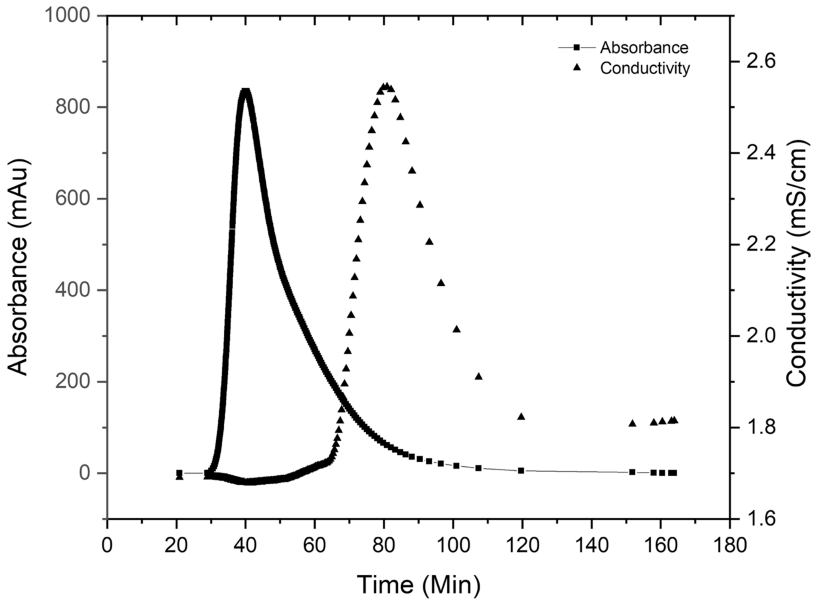


**Figure 2.** SEC chromatogram for *in vitro* refolding of recombinant teriparatide.

**Table 1. Box−Behnken Design for Optimizing *In Vitro* Continuous Refolding Recombinant Teriparatide**

| run no | pattern | feed volume (% CV) | IB concentration (mg/mL) | residence time (min) | refolding yield (%) |
|---|---|---|---|---|---|
| 1 | 0 | 12.5 | 25 | 75 | 95.07 |
| 2 | 0 | 15 | 30 | 75 | 79.16 |
| 3 | 0−+ | 12.5 | 20 | 100 | 83.13 |
| 4 | 0 | 12.5 | 25 | 75 | 92 |
| 5 | −0− | 10 | 25 | 50 | 91.23 |
| 6 | +0− | 15 | 25 | 50 | 92.26 |
| 7 | −+0 | 10 | 30 | 75 | 89.89 |
| 8 | 0++ | 12.5 | 30 | 100 | 92 |
| 9 | 0−− | 12.5 | 20 | 50 | 98.12 |
| 10 | −−0 | 10 | 20 | 75 | 91.41 |
| 11 | 0 | 12.5 | 25 | 75 | 93 |
| 12 | 0+− | 12.5 | 30 | 50 | 76.19 |
| 13 | +−0 | 15 | 20 | 75 | 95.05 |
| 14 | +0+ | 15 | 25 | 100 | 80.63 |
| 15 | −0+ | 10 | 25 | 100 | 89.25 |

analyzed to check the water content using thermogravimetric analysis (TGA). According to the TGA analysis, approximately 60 ± 3.0% of the wet-weight IBs corresponded to water molecules, and the rest of them, 40%, were attributed to IBs.

**3.2. pH-Based Solubilization of Recombinant IBs.** The solubility of IBs directly impacts recombinant protein refolding efficiency. Protein aggregation is among the significant problems associated with higher protein concentration during the solubilized IBs. Non-native hydrophobic interactions between folding intermediates and exposed hydrophobic patches mainly form aggregates. Solubilization of protein aggregates with high concentrations of chaotropic agents creates random-coil structures of proteins with exposed stretches of such hydrophobic amino acids. This increases the tendency for aggregates during refolding. In this study, recombinant teriparatide IBs were solubilized using 20 mM Tris base and 2 mM EDTA at pH 12.5. To minimize the formation of soluble aggregates during the refolding step, the saturation solubility of the IB protein was determined by dissolving variable amounts of IBs in the solubilization buffer. Protein concentration in the samples was determined using absorbance measurements at 280 nm. The maximum solubility of IBs of 30 and 35 mg/mL was obtained at 25.0 °C. In the case of 30 and 35 mg/mL solubilized IBs, we observed a precipitate and no significant increase in absorbance at 280 nm compared to 25 mg/mL. Based on the observed IB solubility behavior, we performed all of the *in vitro* refolding experiments at 20−30 mg/mL IB concentration.

**3.3. Size Exclusion Chromatography-Based Protein Refolding.** The denatured teriparatide IBs were subjected to on-column refolding using size exclusion chromatography, utilizing a buffer with Tris-HCL, EDTA, and arginine at pH 10.5, as shown in Figure 2. The resulting refolded fractions were pooled together to determine the refolding efficiency by using an RP-HPLC-based technique. To overcome these existing challenges of protein refolding using conventional methods, the size exclusion chromatography-assisted refolding method was developed, and the elution behavior of different biomolecules under different SEC conditions was predicted using a general rate model. A multivariate Box−Behnken experimental design was used to achieve the highest possible recovery of refolded biosimilar teriparatide. The effect of three different variables feed volume, IB concentration, and residence time on the refolding yield of recombinant teriparatide was evaluated. Within the selected range of different variables, a higher refolding yield of 98.12% was obtained at feed volume (12% CV), initial IB concentration (20 mg/mL), and residence time (50 min). A mathematical model of the SEC method was developed, considering three mass transfer phenomena within the column: interfacial film mass transfer between the mobile and stationary phases, solute diffusion within the macrospores of the packing particles, and axial dispersion to predict the elution volume. The accuracy of the model predictions was evaluated by comparing them to experimental data. The results showed good agreement between the experimental data and the mathematical model predictions, indicating that the model could accurately predict the elution volume of the size exclusion chromatography process on different scales. There are several limitations of column refolding size exclusion chromatography such as the variability in refolding efficiency among different proteins,


https://doi.org/10.1021/acsomega.3c04463
ACS Omega 2024, 9, 3204−3216

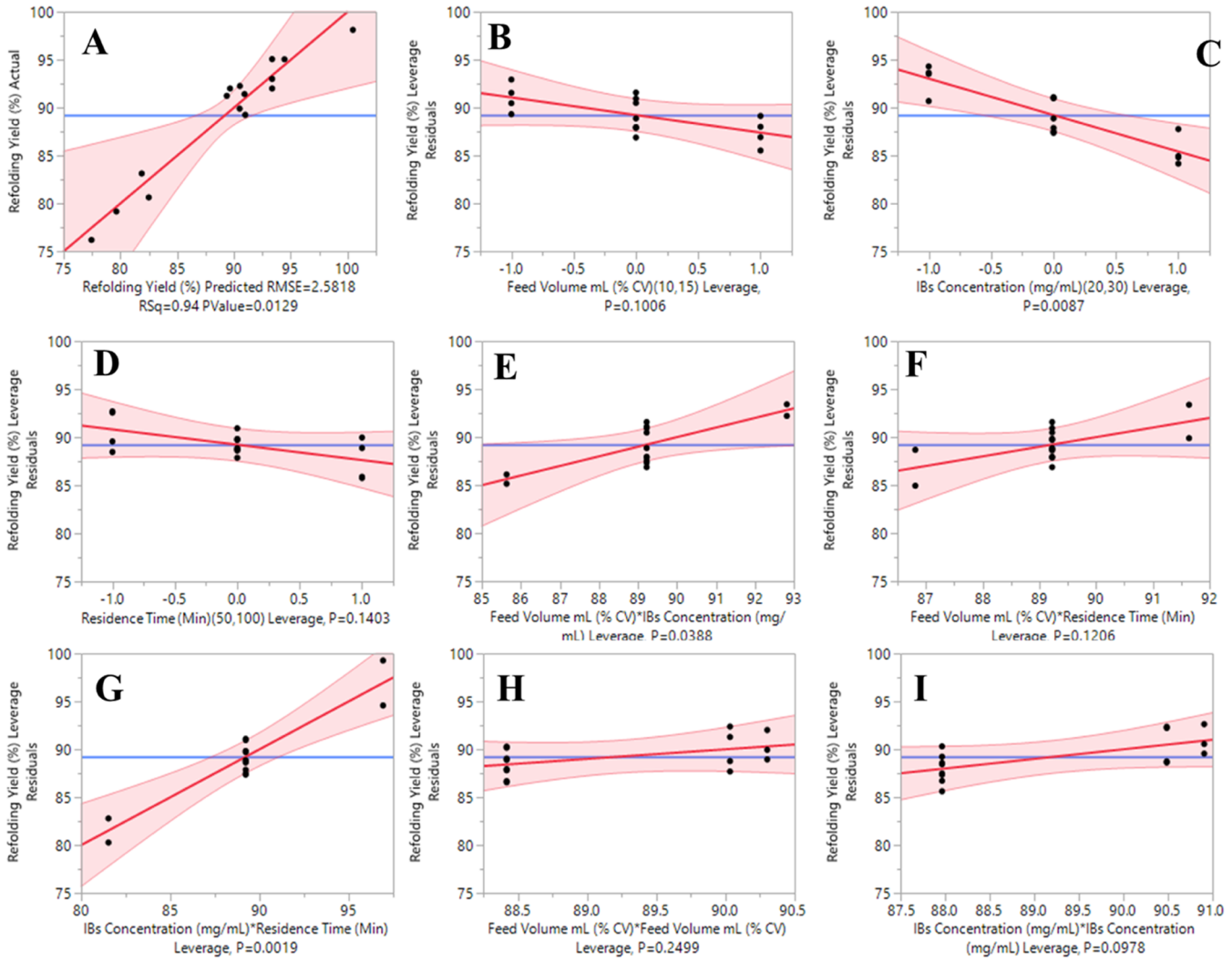


**Figure 3.** (A) Experimental data for % refolding yield against predicted values obtained by the Box−Behnken design. (B−D) Individual effect of variable factors [feed volume (% CV), IB concentration, and residence time on % refolding yield]. (E,G,H,I) Effect of variable factors' mutual interaction on % refolding yield.

especially proteins with complex three-dimensional structures such as antibodies or enzymes having multiple domains with disulfide linkages.

**3.4. Optimization of Refolding of Recombinant Teriparatide.** In this work, we used an integrated strategy and a series of multivariate experiments to establish a novel method for producing recombinant teriparatide from *E. coli* IBs. The parameters and ranges that were examined for each unit operation are shown in Table 1. A multivariate Box−Behnken experimental design was used to determine the significant impact of process parameters on the refolding yield and to find the ideal experimental conditions for refolding recombinant teriparatide. Various parameters were studied, including feed volume (% CV), initial IB concentration (mg/mL), and residence time (min). The reversed-phase HPLC method was developed for biosimilar reference teriparatide to quantify the refolding yield and was supported by reduced SDS-PAGE analysis. Refolding buffer (0.2 M arginine and 0.02 M Tris base, 2 mM EDTA, pH: 10.5) was used with variable refolding residence time, %feed volume, and initial IB concentration as a design center point. The folding yield was evaluated as a function of the above-mentioned three variables. Each set of experiments was performed in two levels of −1 and +1 and included a reference midpoint condition to minimize the variability. The DoE results were analyzed using JMP software and are presented in Figure 3. The DoE results lead to two important conclusions. First, R2 = 0.94 indicates that a quadratic model is acceptable with the simulated results (Figure 3). Second, ANOVA analysis was used to examine the statistical effects of different process factors on the recombinant teriparatide refolding yield. The experimental data agree with model predictions with a root-mean-square error (RMSE) value of 2.5818.

An examination of the estimated parameters indicates that several variables have a statistically significant impact on the refolding efficiency for the refolding of teriparatide using size exclusion chromatography. These variables include refolding residence time, feed volume (% CV), and initial IB concentration (mg/mL), with a significance level of $P \leq 0.02$. IB concentration (mg/mL; $P \leq 0.0087$) significantly influences the refolding efficiency. The P-value of interaction between IB concentration (mg/mL) and residence time (min; $P < 0.0019$) and the P-value of interaction between feed volume (% CV) and IB concentration (mg/mL; $P <$ .03877) were significant, while the residence time was not that statistically significant at $P =$ 0.853 as compared to the other two variables. Figure 4A,B shows


https://doi.org/10.1021/acsomega.3c04463
ACS Omega 2024, 9, 3204−3216

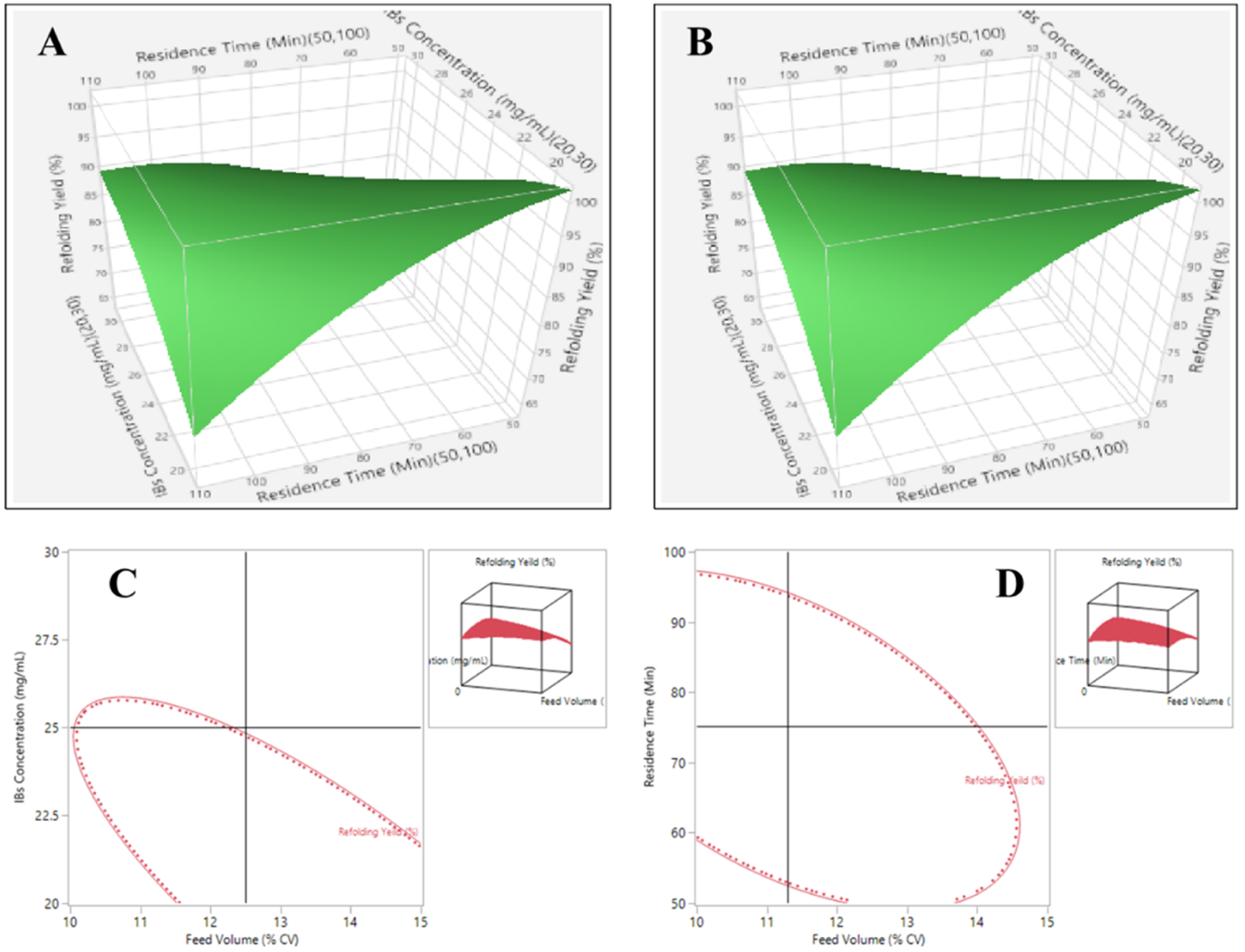


**Figure 4.** Response surface three-dimensional plots showing the effects of variable factors and their mutual interaction on % refolding yield. (A) IB concentration and residence time. (B): IB concentration and feed volume (% CV). (C) Feed volume (% CV) and residence time. (D) Feed volume (% CV) and IB concentration.

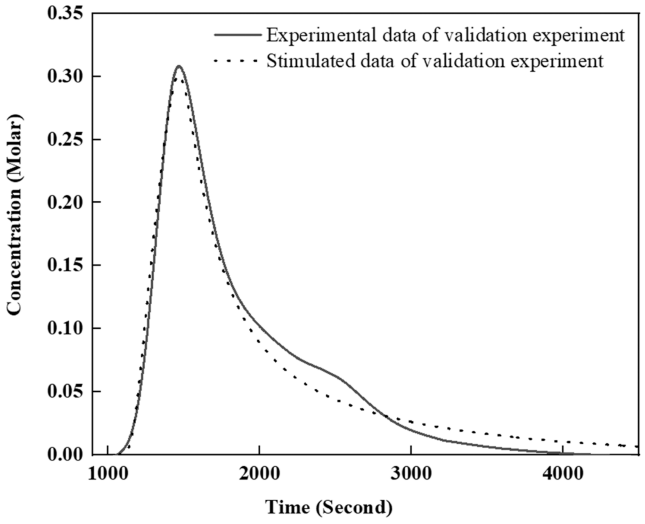


**Figure 5.** Experimental number 1 and simulated chromatograms for SEC-assisted *in vitro* refolding of teriparatide.

three-dimensional response surface plots, showing the effect of the parameters on refolding yield (%). The response surface plot as a 3D surface displayed refolding yield (%) as a function of IB concentration (mg/mL) and residence time (min), feed volume (% CV), and IB concentration (mg/mL) or as a function of feed volume (% CV) and residence time (min). Lower IB concentration and lower percentage column volume load were associated with higher refolding yield.

Further, it was also observed that parameters of the DOE study, namely, % feed volume and IB concentration, significantly impact the refolding of the recombinant teriparatide. Parameter interactions can also be visualized using interaction plots in Supplementary Figure 1. Refolding can be attributed to a decrease in an IB concentration related to an increase in refolding efficiency using size exclusion chromatography. The effect of feed volume (% CV) on refolding yield (%) changes as a decrease in IB concentration and vice versa.

Similarly, the effect of residence time on refolding yield (%) changes the IB concentration and vice versa. The desirability function analysis was used to identify the optimal input parameter combination, resulting in the maximum refolding output. The prediction profiler in Supplementary Figure 2 shows that the optimal parameter combinations for maximizing refold yield were at feed volume (12.5% CV), 25 mg/mL initial IB concentration, and 73 min of residence time with 93.47%


https://doi.org/10.1021/acsomega.3c04463
ACS Omega 2024, 9, 3204−3216

**Table 2. Confirmatory Experiments for Box–Behnken Design Matrix Model Validation and Confirmation and Prediction of Elution Volume Using General Rate Model**

| experiment | feed volume (% CV) | residence time (min) | IB concentration (mg/mL) | refolding yield % (predicted) | refolding yield % (experimental data) | predicted elution volume (mL) | experimental elution volume (mL) |
|---|---|---|---|---|---|---|---|
| 1 | 9 | 80 | 30 | 93.24 | 94.41 | 23.42 | 23.12 |

**Table 3. Estimated Mass Transfer Parameters Estimated by Fitting Experimental Breakthrough curves with GRM**

| sr. no. | model parameters | value |
|---|---|---|
| 1 | $D_{ax}$ ($10^{-8}$ $m^2/s$) | 1.24 ± 0.001 |
| 2 | $K_f$ ($10^{-5}$ m/s) | 3.05 ± 0.001 |
| 3 | $D_p$ ($10^{-12}$ $m^2/s$) | 2.67 ± 0.001 |

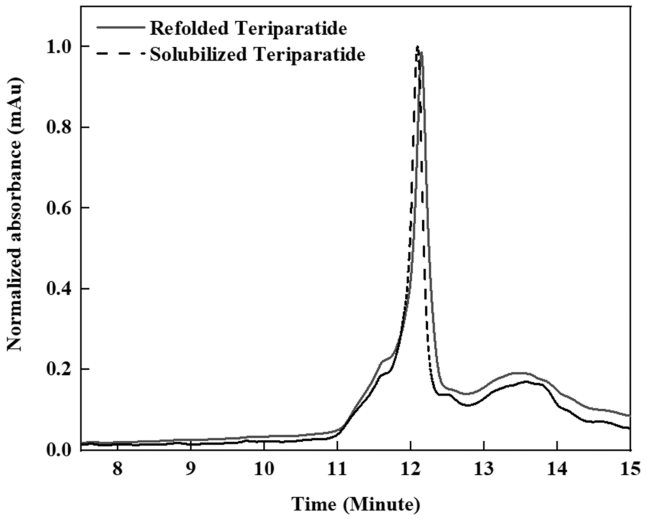


**Figure 6.** RP-HPLC chromatogram for solubilized biosimilar recombinant teriparatide and refolded recombinant teriparatide.

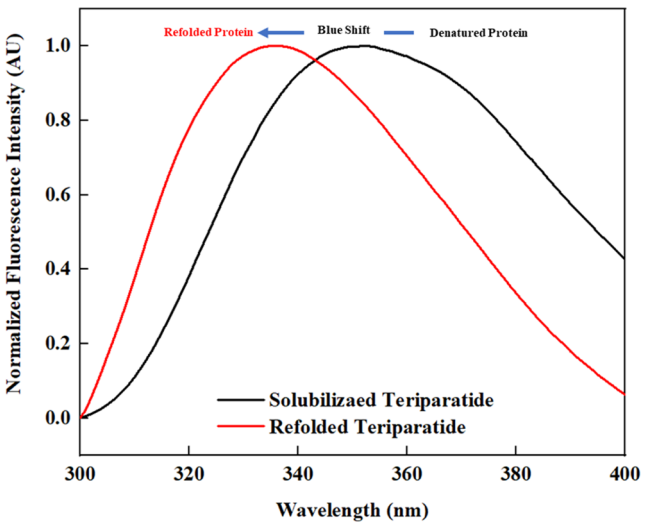


**Figure 7.** Intrinsic fluorescence spectra of refolded and denatured recombinant teriparatide where a blue shift is observed in between the denatured (represented by the black solid line) and refolded protein (represented by the red solid line).

desirability. This shows that as the feed volume (% CV) and initial IB concentration decrease, refolding yield (%) increases. The contour plot shows (Figure 4C,D) the response of two variables at a time (E: feed volume and initial IB concentration, F: initial IB concentration and residence time.).

**3.5. Validation of the SEC-Based Recombinant Teriparatide Refolding Model.** To test for repeatability and validate the model, a single run was carried out for the optimal values acquired from the model. Validation experiments were conducted using the following prediction expression post optimization of experimental conditions for a higher refolding yield. An FPLC chromatogram showing the protein elution of size exclusion chromatography is shown in Figure 5.

$$\begin{aligned}\text{Refoldingyield \%} = {} & 93.35 + -1.83 * \left(\frac{(\%\ \text{CV load} - 12.5)}{2.5}\right) + -3.80 * \left(\frac{(\text{IB concentration} - 25)}{5}\right) + -1.59 * \left(\frac{(\text{Residence time} - 75)}{25}\right) \\ & + \left(\frac{(\%\ \text{CV load} - 12.5)}{2.5}\right) * \left(\left(\frac{(\text{IB concentration} - 25)}{5}\right) * - 3.59\right) \\ & + \left(\frac{(\%\ \text{CV load} - 12.5)}{2.5}\right) * \left(\left(\frac{(\text{Residence time} - 75)}{25}\right) * - 2.41\right) \\ & + \left(\frac{(\text{IB concentration} - 25)}{5}\right) * \left(\left(\frac{(\text{Residence time} - 75)}{25}\right) * 7.7\right) \\ & + \left(\frac{(\%\ \text{CV load} - 12.5)}{2.5}\right) * \left(\left(\frac{(\%\ \text{CV load} - 12.5)}{2.5}\right) * - 1.74\right) \\ & + \left(\frac{(\text{IB concentration} - 25)}{5}\right) * \left(\left(\frac{(\text{IB concentration} - 25)}{5}\right) * - 2.73\right) \\ & + \left(\frac{(\text{Residence time} - 75)}{25}\right) * \left(\left(\frac{(\text{Residence time} - 75)}{25}\right) * - 3.26\right)\end{aligned}$$



https://doi.org/10.1021/acsomega.3c04463
ACS Omega 2024, 9, 3204–3216

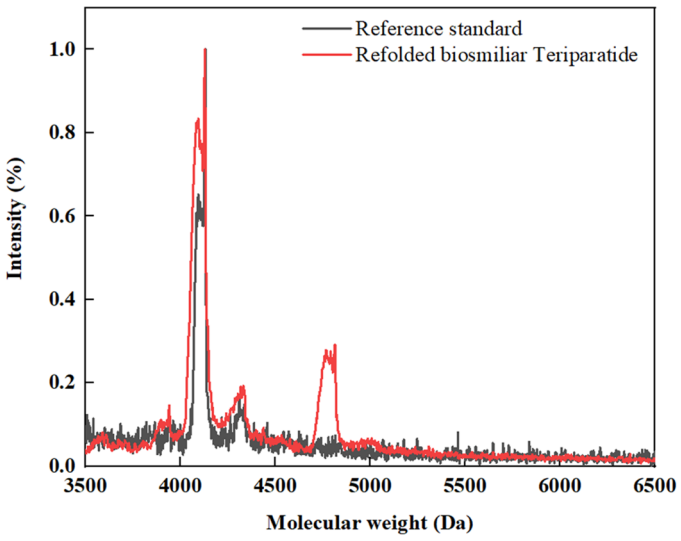


(A)

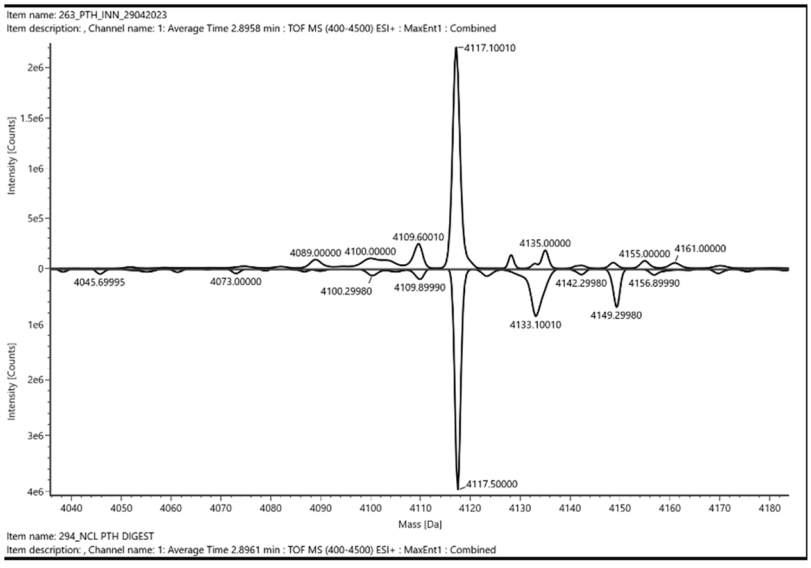


(B)

**Figure 8.** (A) Intact mass analysis of refolded recombinant teriparatide and reference standard analyzed by MALDI-TOF. (B) LC-ESI-MS/MS deconvoluted spectra showing the intact mass of refolded recombinant teriparatide and reference standard.

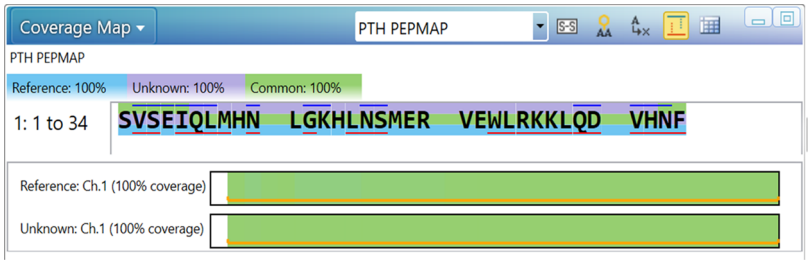


**Figure 9.** Amino acid sequence of recombinant teriparatide and their coverage map analyzed using LC-ESI-MS/MS.

The sign of each coefficient in the prediction formula denotes the sign of the relationship between a predictor variable and a responder variable. In the prediction equation, a positive sign of the coefficient means that as the predictor variable increases, the response variable increases, whereas a negative sign indicates that as the predictor variable increases, the response variable decreases. The higher the refolding dilution, the better the refolding yield, according to a positive coefficient value for the fold dilution. Table 2 compares the model-predicted and experimental values for the optimum conditions and shows the RMSD value for the runs performed. When compared to the actual experimental data, the model's predictions for refolding yield (RMSD < 2.58%) can be observed.



https://doi.org/10.1021/acsomega.3c04463
ACS Omega 2024, 9, 3204−3216

**3.6. Parameter Estimation Using a Model Fitting to the Experimental On-Column Refolding of Teriparatide Using SEC.** The on-column refolding using size exclusion chromatography experiments for recombinant teriparatide (PTH-34) were performed at three different residence times 50, 75, and 100 min for Sephadex G-25 resin at three different initial teriparatide IB concentrations and feed volumes (% CV), i.e., 20, 25, and 30 mg/mL and 10%, 12.5%, and 15%, respectively. The experimental on-column refolding elution chromatograms at 80 min residence time, 9% CV feed volume, and $C_0$ of 30 mg/mL, as shown in Figure 2, were used for the inverse fitting to estimate mass transfer parameters in size exclusion chromatography. The estimated mass transfer parameters with confidential intervals are listed in Table 3. The experimental data for the prediction of elution volume were found to be in good agreement with model predictions with *R*-squared ($R^2$) values of greater than 0.99 for each experiment. The experimental and simulated breakthrough curves are shown in Figure 5. A simulated elution profile can be used to predict the process design space for the on-column refolding of peptides using size exclusion chromatography by exploring the various operating conditions such as IB concentration, feed volume, and residence time. A good agreement between the experimental and simulated chromatograms shows the effectiveness of the developed hybrid protocol in predicting and validating the performance of *in vitro* SEC-based refolding.

**3.7. Analytical Characterization of Refolded Recombinant Teriparatide.** The characterization of the refolded recombinant teriparatide was carried out by using various orthogonal analytical techniques. By using reducing SDS-PAGE, the initial expression of the recombinant teriparatide and refolding are observed in Figure 1B. The refolded recombinant teriparatide moved with a predicted mobility of 4.1 kDa under reducing conditions. To confirm the three-dimensional structure of the refolded recombinant teriparatide, an internal reference standard recombinant teriparatide and an in-house refolded teriparatide were investigated as a control. The RP-HPLC chromatogram indicates the hydrophobicity behavior of refolded recombinant teriparatide and solubilized teriparatide (Figure 6).

In this study, we used the intrinsic fluorescence of aromatic amino acids to determine the higher-order structure of denatured and refolded proteins. The intrinsic fluorescence spectra of the solubilized and refolded protein showed a blue shift initially. Figure 7 displays the $\lambda$-max for the solubilized protein as 352 ± 0.5 nm, while for the refolded protein, it is 335 ± 1.0 nm. We compared the intact masses of the reference standard and the purified refolded recombinant teriparatide. The intact mass of reference standard teriparatide (BONMAX PTH CARTRIDGE 100 IU, ZYDUS) was 4117.1 ± 0.2 Da, while the intact mass of the recombinant teriparatide was 4117.5 ± 0.5 Da (Figure 8A,B). We used liquid chromatography-electrospray ionization-tandem mass spectrometry (LC-ESI-MS/MS) to examine the amino acid sequence of recombinant teriparatide, comparing it to a reference standard. Using MS-based peptide mapping, we obtained a complete sequence coverage map for both molecules, as shown in Figure 9, examining various aspects such as the observed *m*/*z*, miscleavage, charge state, and retention time of the matched fragment ions and their annotations, as shown in Supplementary Tables 1 and 2, for recombinant teriparatide and reference standard, respectively. Peptide mapping of the digested protein gives detailed information about the primary sequence, and mapped MS peptides are documented in Supplementary Figures 3 and 4.

## 4. CONCLUSIONS

A time- and cost-efficient SEC-assisted *in vitro* refolding process for recombinant teriparatide was developed. The developed platform offers several advantages over existing dilution-assisted protein refolding, such as higher productivity, lower process time and cost, and improved product quality with a lower aggregate level. DOE-based empirical optimization of SEC-based refolding shows that the feed volume (% CV) and IB concentration (mg/mL) are the most critical process parameters affecting the overall refolding yield. We have also developed the GRM-based modeling platform to predict the performance of the SEC-assisted protein refolding. The developed model helped in the accurate prediction of the elution volume and refolding yield of the SEC-assisted *in vitro* refolding process. Fluorescence and mass analyses confirm the structural integrity of the refolded peptide. Intact mass analysis and peptide fingerprinting also confirm the biosimilarity to the reference standard teriparatide molecule. The developed protocol here is a valuable tool for designing high-yield, scalable refolding protocols for recombinant peptides without disulfide bonds.

## ■ ASSOCIATED CONTENT

### Supporting Information

The Supporting Information is available free of charge at https://pubs.acs.org/doi/10.1021/acsomega.3c04463.

Supporting Information is included in the form of figures and tables as supporting data: Interaction profile of refolding variable factors such as feed volume (% CV), IB concentration, and retention time on the % refolding yield. Prediction profile for the effect of feed volume (% CV), IB concentration, and residence time on the refolding yield (%). MS/MS profile of the recombinant teriparatide peptide with different fragment ions (b and y) in CID mode. MS/MS profile of the reference standard teriparatide peptide with different fragment ions (b and y) in CID mode (PDF)

## ■ AUTHOR INFORMATION


### Corresponding Author

**Rahul Bhambure** − *Chemical Engineering and Process Development Division, CSIR - National Chemical Laboratory, Pune 411008, India; Academy of Scientific and Innovative Research (AcSIR), Ghaziabad 201002, India;* orcid.org/0000-0003-4402-5739; Phone: +9120-2590-2318; Email: rs.bhambure@ncl.res.in

### Authors

**Santosh Ughade** − *Chemical Engineering and Process Development Division, CSIR - National Chemical Laboratory, Pune 411008, India; Academy of Scientific and Innovative Research (AcSIR), Ghaziabad 201002, India*

**Sunil Rana** − *Chemical Engineering and Process Development Division, CSIR - National Chemical Laboratory, Pune 411008, India; Academy of Scientific and Innovative Research (AcSIR), Ghaziabad 201002, India*

**Mohd Nadeem** − *Chemical Engineering and Process Development Division, CSIR - National Chemical Laboratory, Pune 411008, India; Indian Institute of Technology Bombay, Mumbai 400076, India*




https://doi.org/10.1021/acsomega.3c04463
ACS Omega 2024, 9, 3204−3216

**Rupali Kumthekar** − *Chemical Engineering and Process Development Division, CSIR - National Chemical Laboratory, Pune 411008, India; Academy of Scientific and Innovative Research (AcSIR), Ghaziabad 201002, India*

**Sanjay Mahajani** − *Chemical Engineering and Process Development Division, CSIR - National Chemical Laboratory, Pune 411008, India; Indian Institute of Technology Bombay, Mumbai 400076, India;* orcid.org/0000-0001-7090-4097

Complete contact information is available at: https://pubs.acs.org/10.1021/acsomega.3c04463

### Author Contributions

S.U. and S.R. contributed equally to this work. S.U., S.R., and R.B. designed the experiments. S.U., S.R., and R.K. performed the experiments. M.N., S.M., and R.B. developed and validated the SEC chromatography model. S.U., S.R., R.K., M.N., and R.B. analyzed the results. R.B. supervised the project and was the recipient of the funding. All authors were involved in the drafting, review, and approval of the report and the decision to submit it for publication.

### Notes

The authors declare no competing financial interest.

## ■ ACKNOWLEDGMENTS

The authors are grateful for the financial support to this research work by the Department of Biotechnology, Govt. of India DST-DPRP (grant no. VI-D&P/564/2016-2017/TDT(G): GAP322726, and BT/NBM0161/04/19). S.U. acknowledges a senior research fellowship from UGC-SRF [ref No.:838/(CSIR-UGC NET JUNE 2018)]. S.R. acknowledges a senior research fellowship from UGC-SRF [ref No. 427/ (CSIR-UGC NET JUNE 2018)]. M.N. acknowledges a PM fellowship (PMRF ID: 1300743). R.K. acknowledges a senior research fellowship from CSIR-SRF [ref No. 17/12/2017(ii) EU-V]. The authors are grateful for technical support with CADET-based model development from Prof. Eric von Lieres, Institute of Biotechnology, Forschungszentrum Jülich, Germany.

## ■ ABBREVIATIONS

SEC, size exclusion chromatography; IBs, inclusion bodies; CHO, Chinese hamster ovary cells; NSO, non-secreting murine myeloma cells; mAbs, monoclonal antibodies; *E. coli*, *Escherichia coli*; IgG, immunoglobulin G; GRM, general rate model; Dax, axial dispersion coefficient; Kf, film mass transfer coefficient; Dp, pore diffusion coefficient; TB, Tartoff−Hobbs HiVeg broth; OD600 nm, optical density at 600 nm; IPTG, isopropyl $\beta$58 d-1-thiogalactopyranoside; SDS-PAGE, sodium dodecyl sulfate-polyacrylamide gel electrophoresis; MALDI/TOF, matrix-assisted laser desorption ionization/time of flight; RP-HPLC, reversed-phase high-performance liquid chromatography; LC-ESI-MS/MS, liquid chromatography-electrospray ionization-tandem mass spectroscopy; CID, collision-induced dissociation; Glu-C, endoproteinase Glu-C sequencing grade; VL16, Vantage L Laboratory Column VL 16 × 250

## ■ REFERENCES

(1) Lamers, C. Overcoming the Shortcomings of Peptide-Based Therapeutics. *Future Drug Discovery* **2022**, *4* (2), FDD75.

(2) Wang, L.; Wang, N.; Zhang, W.; Cheng, X.; Yan, Z.; Shao, G.; Wang, X.; Wang, R.; Fu, C. Therapeutic Peptides: Current Applications and Future Directions. *Sig. Transduct. Target. Ther.* **2022**, *7* (1), 48.

(3) Banting, F. G.; Best, C. H.; Collip, J. B.; Campbell, W. R.; Fletcher, A. A. Pancreatic Extracts in the Treatment of Diabetes Mellitus. *Can. Med. Assoc J.* **1922**, *12* (3), 141−146.

(4) Lubell, W. D. Peptide-Based Drug Development. *Biomedicines* **2022**, *10* (8), 2037.

(5) Lau, J. L.; Dunn, M. K. Therapeutic Peptides: Historical Perspectives, Current Development Trends, and Future Directions. *Bioorg. Med. Chem.* **2018**, *26* (10), 2700−2707.

(6) Lee, A. C.-L.; Harris, J. L.; Khanna, K. K.; Hong, J.-H. A Comprehensive Review on Current Advances in Peptide Drug Development and Design. *Int. J. Mol. Sci.* **2019**, *20* (10), 2383.

(7) Craik, D. J.; Kan, M.-W. How Can. We Improve Peptide Drug Discovery? Learning from the Past. *Expert Opin. Drug Discovery* **2021**, *16* (12), 1399−1402.

(8) Otvos, L.; Wade, J. D. Current Challenges in Peptide-Based Drug Discovery. *Front. Chem.* **2014**, *2*, 62 DOI: 10.3389/fchem.2014.00062.

(9) Ferrer-Miralles, N.; Domingo-Espín, J.; Corchero, J. L.; Vázquez, E.; Villaverde, A. Microbial Factories for Recombinant Pharmaceuticals. *Microb. Cell Fact.* **2009**, *8* (1), 17.

(10) Makrides, S. C. Strategies for Achieving High-Level Expression of Genes in *Escherichia Coli*. *Microbiol. Rev.* **1996**, *60* (3), 512−538.

(11) Francis, D. M.; Page, R. Strategies to Optimize Protein Expression in *E. Coli*. *Curr. Protoc. Protein Sci.* **2010**, *61* (1), 5241−52429.

(12) Choi, J. H.; Keum, K. C.; Lee, S. Y. Production of Recombinant Proteins by High Cell Density Culture of *Escherichia Coli*. *Chem. Eng. Sci.* **2006**, *61* (3), 876−885.

(13) Carrió, M.; Villaverde, A. Protein Aggregation as Bacterial Inclusion Bodies Is Reversible. *FEBS Lett.* **2001**, *489* (1), 29−33.

(14) Singh, A.; Upadhyay, V.; Upadhyay, A. K.; Singh, S. M.; Panda, A. K. Protein Recovery from Inclusion Bodies of *Escherichia Coli* Using Mild Solubilization Process. *Microb. Cell Fact.* **2015**, *14* (1), 41.

(15) Rehm, B. H. A.; Qi, Q.; Beermann, B. B.; Hinz, H. J.; Steinbüchel, A. Matrix-Assisted *in Vitro* Refolding of Pseudomonas Aeruginosa Class II Polyhydroxyalkanoate Synthase from Inclusion Bodies Produced in Recombinant *Escherichia Coli*. *Biochem. J.* **2001**, *358* (Pt 1), 263−268.

(16) Li, F.; Dong, P.-J.; Zhuang, Q.-F. Novel Column-Based Protein Refolding Strategy Using Dye-Ligand Affinity Chromatography Based on Macroporous Biomaterial. *J. Chromatogr. A* **2009**, *1216* (20), 4383−4387.

(17) Nabiel, A.; Yosua, Y.; Sriwidodo, S.; Maksum, I. P. Overview of Refolding Methods on Misfolded Recombinant Proteins from *Escherichia Coli* Inclusion Bodies. *J. Appl. Biol. Biotech.* **2022**, *11*, 47−52, DOI: 10.7324/JABB.2023.112204.

(18) Feng, Y.; Zhang, M.; Zhang, L.; Zhang, T.; Ding, J.; Zhuang, Y.; Wang, X.; Yang, Z. An Automatic Refolding Apparatus for Preparative-Scale Protein Production. *PLoS One* **2012**, *7* (9), No. e45891.

(19) Gani, K.; Bhambure, R.; Deulgaonkar, P.; Mehta, D.; Kamble, M. Understanding Unfolding and Refolding of the Antibody Fragment (Fab). I. In-Vitro Study. *Biochem. Eng. J.* **2020**, *164*, No. 107764.

(20) Jungbauer, A.; Kaar, W. Current Status of Technical Protein Refolding. *J. Biotechnol.* **2007**, *128* (3), 587−596.

(21) Chen, S.; Wellborn, W. B.; Cundy, J. T.; Mangalath-Illam, R.; Cook, S. A.; Stork, M. J.; Martin, J. P.; Caparon, M. H.; Sobacke, S. E.; Srinivasan, S.; Quaadgras, J. P. Chapter 38 - Process Development and Intensification for a Recombinant Protein Expressed in *E. coli*. In *Biopharmaceutical Processing*; Jagschies, G.; Lindskog, E.; Łącki, K.; Galliher, P., Eds.; Elsevier, 2018; pp 769−791.

(22) Linke, T.; Aspelund, M. T.; Thompson, C.; Xi, G.; Fulton, A.; Wendeler, M.; Pabst, T. M.; Wang, X.; Wang, W. K.; Ram, K.; Hunter, A. K. Development and Scale-up of a Commercial Fed Batch Refolding Process for an Anti-CD22 Two Chain Immunotoxin. *Biotechnol. Prog.* **2014**, *30* (6), 1380−1389.

(23) Jungbauer, A.; Kaar, W.; Schlegl, R. Folding and Refolding of Proteins in Chromatographic Beds. *Curr. Opin. Biotechnol.* **2004**, *15* (5), 487−494.

(24) Li, M.; Su, Z.-G.; Janson, J.-C. In Vitro Protein Refolding by Chromatographic Procedures. *Protein Expr. Purif.* **2004**, *33* (1), 1−10.

(25) Rajendran, V.; Ponnusamy, A.; Pushpavanam, S.; Jayaraman, G. Continuous Protein Refolding and Purification by Two-Stage Periodic Counter-Current Chromatography. *J. Chromatogr. A* **2023**, *1695*, No. 463938.
(26) Batas, B.; Chaudhuri, J. B. Protein Refolding at High Concentration Using Size-Exclusion Chromatography. *Biotechnol. Bioeng.* **1996**, *50* (1), 16−23.
(27) Gao, Y.-g.; Guan, Y.; Yao, S.; Cho, M. Lysozyme Refolding at High Concentration by Dilution and Size-Exclusion Chromatography. *J. Zhejiang Univ. Sci. A* **2003**, *4* (2), 136−141.
(28) Saremirad, P.; Wood, J. A.; Zhang, Y.; Ray, A. K. Oxidative Protein Refolding on Size Exclusion Chromatography: From Batch Single-Column to Multi-Column Counter-Current Continuous Processing. *Chem. Eng. Sci.* **2015**, *138*, 375−384.
(29) Wang, C.; Cheng, Y. Urea-Gradient Protein Refolding in Size Exclusion Chromatography. *Curr. Pharm. Biotechnol.* **2010**, *11* (3), 289−292.
(30) Gu, Z.; Su, Z.; Janson, J. C. Urea Gradient Size-Exclusion Chromatography Enhanced the Yield of Lysozyme Refolding. *J. Chromatogr A* **2001**, *918* (2), 311−318.
(31) Chaudhuri, J. B.; Fahey, E. *Use of Size-Exclusion Chromatography for Refolding Recombinant Proteins from Inclusion Bodies*, Abstracts of Papers, 221st ACS National Meeting, San Diego, CA, United States, April 1−5, 2001, 2001, BIOT-031.
(32) Enna, S. J.; Bylund, D. B. Teriparatide. In *xPharm: The Comprehensive Pharmacology Reference*; Enna, S. J.; Bylund, D. B., Eds.; Elsevier: New York, 2007; pp 1−2.


https://doi.org/10.1021/acsomega.3c04463
*ACS Omega* 2024, 9, 3204−3216